Clays and Clay Minerals, Vol. 52, No. 5, 635–642, 2004.

DEHYDRATION AND REHYDRATION OF PALYGORSKITE AND THE INFLUENCE OF WATER ON THE NANOPORES

WENXING KUANG, GLENN A. FACEY AND CHRISTIAN DETELLIER*

Center for Catalysis Research and Innovation and Department of Chemistry, University of Ottawa, Ottawa, Ontario, Canada K1N 6N5

Abstract—The dehydration and rehydration processes of the clay mineral palygorskite (PFl-1) were studied by textural analysis, thermogravimetric analysis connected with mass spectrometry (TGA-MS), and ^{29}Si and ^{1}H solid-state NMR techniques. The TGA-MS results clearly reveal weight losses at maxima of 70ºC, 190ºC, 430ºC and 860ºC. PFl-1 is characterized by a micropore area of 93 m^2/g, corresponding to a micropore volume of 47 mm^3/g. These values are also obtained for the sample heated up to 200ºC for 20 h. Further heating at 300ºC produces a collapse of the structure, as shown by the almost complete loss of microporosity.

The ^{29}Si NMR spectra of palygorskite show two main resonances at −92.0 and −97.5 ppm, attributed to one of the two pairs of equivalent Si nuclei in the basal plane. A minor resonance at −84.3 ppm is attributed to Q^2(Si-OH) Si nuclei. The resonance at −92.0 ppm is assigned to the central Si position, while the resonance at −97.5 ppm is assigned to the edge Si sites. It is confirmed by solid-state ^{29}Si and ^{1}H NMR that nearly complete rehydration is achieved by exposing palygorskite samples that have been partially dehydrated at 150ºC and 300ºC, to D_2O or water vapor at room temperature. When the rehydration is accomplished with D_2O, the atoms are disordered across all the protons sites.

Key Words—Clay Minerals, Microporosity, Palygorskite, Sepiolite, Textural Analysis, TGA-MS, ^{29}Si NMR.

INTRODUCTION

Palygorskite is an important clay mineral with industrial applications, due to its unique crystal structure and microfibrous nature (Serratosa, 1979; Jones and Galán, 1988; Galán, 1996). The name palygorskite was first used by von Ssaftschenkov in 1862, from the name of the locality where it was first found, Palygorsk (Jones and Galán, 1988, and references therein). A fascinating application of palygorskite was its use centuries ago by the Mayas to prepare a blue pigment known as 'Maya Blue' (van Olphen, 1966; Kleber *et al*., 1967; Yacamán *et al*., 1996; Polette *et al*., 2002; Chiari *et al*., 2003; Fois *et al*., 2003; Hubbard *et al*., 2003).

Palygorskite and sepiolite are 2:1 type phyllosilicates (Jones and Galán, 1988, and references therein). The structure of palygorskite is derived from talc-like T-O-T ribbons that expand along the axis of the fibers, with a width of two pyroxene chains. The octahedral sites are principally occupied by Mg(II) cations, with some replacement principally by Al(III) or Fe(III) cations. Each ribbon is connected to the next through an inverted Si−O−Si bond, resulting in a continuous tetrahedral sheet and a discontinuous octahedral sheet. Rectangular, tunnel-like nanopores are formed. The terminal cations that are located at the edges of the octahedral sheets complete their coordination shells with two molecules of water, the structural water. The nanopores run parallel to the fiber axis and are filled at room temperature by zeolitic water molecules that are hydrogen bonded to the structural water. The zeolitic water is easily lost at relatively low temperature, <120ºC. The cross-sections of the tunnels are ~3.7 × 6.4 Å. They are responsible for the large specific surface area and excellent sorptive properties of palygorskite, once the zeolitic water has been removed by thermal treatment.

Besides the monoclinic structure model for palygorskite (Bradley, 1940; Preisinger, 1963), an orthorhombic structure model has also been proposed (Chisholm, 1990, 1992; Artioli and Galli, 1994; Artioli *et al*., 1994; Chiari *et al*., 2003). An intermediary structure between dioctahedral and trioctahedral has been proposed (Galán and Carretero, 1999). Recently, Chahi *et al*. (2002) found evidence of trioctahedral Mg_3OH features.

Palygorskite is progressively dehydrated with increase in temperature (Preisinger, 1963). Heating palygorskite in air at relatively low temperatures removes selectively water adsorbed on external surfaces and the zeolitic water from the nanoporous tunnels, while leaving the structural water and the Mg-OH groups unaffected. The elimination of coordinated, structural water starts when the zeolitic water is lost and ends when dehydroxylation begins. Folding of the palygorskite crystals occurs when some structural water has been removed, which allows the terminal Mg(II) to complete its coordination with the oxygen of the neighboring silica surface. Structural folding is nearly completely reversible provided that the treatment temperature does

* E-mail address of corresponding author:
dete@science.uottawa.ca
DOI: 10.1346/CCMN.2004.0520509

not exceed 350ºC, but becomes irreversible once all the structural water molecules are removed and partial dehydroxylation has occurred, forming an anhydride form. Finally, the remaining Mg-OH hydroxyl groups are released at ~850ºC (VanScoyoc *et al*., 1979; Frost and Ding, 2003).

Given the large number of applications of palygorskite (Murray, 1991, 1999, 2000), it is of great interest to fully characterize and to understand its properties. In recent years, there have been numerous studies of palygorskite (*e.g*. Augsburger *et al*., 1998; Frost *et al*., 1998, 2001; Fernandez *et al*., 1999; Galán and Carretero, 1999; Borden and Giese, 2001; Madejová and Komadel, 2001; Wu, 2001; Birsoy, 2002; Chahi *et al*., 2002; McKeown *et al*., 2002; Sidheswaran, 2002). A variety of physicochemical techniques such as X-ray diffraction (XRD), thermal analysis, infrared (IR) spectroscopy, solid-state nuclear magnetic resonance (NMR) spectroscopy, scanning electron microscopy (SEM) and textural analysis have been performed to characterize palygorskite (Jones and Galán, 1988; Costanzo and Guggenheim, 2001),

There are some contradictory reports in the literature, *e.g*. the assignment for the resonances in the ^{29}Si NMR spectrum of palygorskite (Barron and Frost, 1985; Komarneni *et al*., 1986; d'Espinose de la Caillerie and Fripiat, 1994), the BET surface area determined from textural analysis, which can range from 50−83 m^2/g to 222 m^2/g for palygorskite (PFl-1) (van Olphen and Fripiat, 1979; Shariatmadari, *et al*., 1999) and thermal analysis (Jones and Galán, 1988; Shuali *et al*., 1988, 1990; Frost and Ding, 2003).

In previous studies, the ^{29}Si MAS NMR spectrum of sepiolite was assigned using cross-polarization techniques (Barron and Frost, 1985; Sanz, 1990) and two-dimensional ^{1}H-^{29}Si HETCOR and ^{29}Si-COSY pulse sequences (Shore *et al*., 1998; Weir *et al*., 2002). As sepiolite and palygorskite are chemically and structurally similar, differing mainly by the length of their unit-cell, the previous results from sepiolite are helpful for the peak assignments of palygorskite. In the current work, the ^{29}Si MAS and CP/MAS NMR spectra of palygorskite were analyzed at room temperature and upon thermal treatment. It is also confirmed by solid-state NMR that nearly complete rehydration is achieved at room temperature by exposing palygorskite samples that had been partially dehydrated up to 300ºC to D_2O or H_2O vapor.

EXPERIMENTAL

Materials

Palygorskite (PFl-1) from Gadsden County, Florida, was obtained from the Source Clays Repository of the Clay Minerals Society (Purdue University), with a chemical composition (%) of SiO_2 (60.35), Al_2O_3 (11.13), Fe_2O_3 (3.74), TiO_2 (0.48), MgO (10.58), CaO (1.89), Na_2O (0.05), K_2O (0.87), P_2O_5 (0.92) (Mermut and Cano, 2001); structure: $(Mg_{0.33}Ca_{0.62}Na_{0.04}K_{0.13})[Al_{1.50}Fe^{3+}_{0.52}Fe^{2+}_{0.01}Mn_{0.01}Mg_{1.91}Ti_{0.06}][Si_{7.88}Al_{0.22}]O_{20}(OH)_4$. As reported by Güven *et al*. (1992), palygorskite makes up ~85% of the fine (<2 μm) fraction. Smectite (10%), quartz (1−3%), apatite (2%), carbonates (1%) and mica (<1%) were identified as the main impurities in the fine fraction. These data are close to those reported by Chipera and Bish (2001).

Deuterium oxide (>99.9%) was obtained from Cambridge Isotope Laboratories, Inc.

Rehydration of samples

Palygorskite was heated with a ramp rate of 1ºC/min to 150ºC (or 300ºC) and then kept at 150ºC (or 300ºC) for 20 h under air in a baffle furnace to eliminate selectively the surface-bound water, and zeolitic water (and partially structural water) from the nanoporous tunnels. The vials containing ~0.1 g of the partially dehydrated palygorskite were immediately transferred from the furnace into capped bottles containing a few mL of water or D_2O and then remained in contact with the vapor at room temperature.

Nuclear magnetic resonance spectroscopy

Solid-state ^{1}H magic-angle spinning (MAS) NMR, and ^{29}Si MAS and cross-polarization (CP)/MAS NMR spectra were recorded at 200.10 and 39.75 MHz, respectively, at room temperature, on a Bruker ASX-200 spectrometer. Typical spinning rates of 6 kHz (^{1}H) and 4 kHz (^{29}Si) were used. The excitation pulse and recycle time for ^{1}H NMR were 3.5 μs (π/2 pulse) and 2 s (16 scans), respectively. A ramped CP pulse sequence was used for all ^{29}Si cross-polarization experiments. The recycle delay time was 2 s, which was found to be adequate for proton relaxation based on proton MAS signal intensity measured as a function of delay time. The proton 90º pulse was 4 μs. The contact time to allow the transfer of magnetization between ^{1}H and ^{29}Si nuclei was 10 ms. The direct ^{29}Si MAS spectra were collected using 4 μs pulses (90 deg) and high-power proton decoupling. The recycle delay was 2 s. The ^{1}H NMR signals were externally referenced to the $-CH_3$ resonance of acetone at 2.06 ppm, corresponding to tetramethylsilane (TMS) at 0 ppm. The ^{29}Si NMR signals were externally referenced to the $-Si(CH_3)_3$ resonance of tetrakis trimethylsilylsilane at −9.9 ppm, corresponding to TMS at 0 ppm.

Thermal analysis

Differential thermal analysis (DTA), thermogravimetric analysis (TGA), and derivative thermal gravimetric (DTG) analysis were performed on a TA SDT 2960 instrument. Approximately 10−20 mg samples were placed in a platinum crucible on the pan of a microbalance, and then heated from room temperature to 1000ºC at a heating rate of 10ºC/min while being purged

https://doi.org/10.1346/CCMN.2004.0520509 Published online by Cambridge University Press

with He at a flow rate of 100 mL/min and constantly weighed. The gases were drawn down a capillary in the SDT furnace. Mass spectra were recorded on a Pfeiffer GSD 301 instrument. The mass spectrum was run in the scanning mode from mass 10 to mass 80, at a scan rate of 0.2 s per mass.

Texture analysis

The BET surface area and micropore measurements were performed on a Micromeritics ASAP-2010 instrument (N_2 or Ar adsorption at −196ºC). The samples were pre-degassed at room temperature under vacuum on the apparatus. The degas process was terminated when the vacuum pressure decreased to 3 μm Hg. The molecular cross-section of N_2 used in the data analysis was 0.1620 nm^2. The typical range of thickness chosen for t-plot measurements was 3.5 to 5 Å.

RESULTS AND DISCUSSION

Structure of palygorskite

Four major weight-loss steps were observed on the TGA curve for palygorskite in the range of temperatures from room temperature to 1000ºC in He gas. These steps are similar to the thermal behavior of palygorskite under N_2 (Guggenheim and Koster van Groos, 2001; Frost and Ding, 2003). The four steps, which correspond to weight losses of 4.8% (room temperature to 130ºC), 3.3% (130−270°C), 5.1% (270−580°C), and 1.2% (580−950ºC), were assigned to the release of zeolitic water, the release of the first structural water, the release of the second structural water, and the dehydroxylation of the Mg-OH groups, respectively (Shuali *et al*., 1988). This is in agreement with the *in situ* mass spectrometry analysis: gaseous water is evolved from the material at the same temperatures. Figure 1 shows the corresponding DTG and mass spectrometric analyses of water. It is interesting to note that the DTG curve is almost identical to the water mass trace. Similar results were reported for PFl-1 (Frost and Ding, 2003) or for palygorskite samples from other origins (Shuali *et al*., 1990; Artioli *et al*., 1994). Four major weight-loss events are clearly observed at maxima of 70ºC, 190ºC, 430ºC and 860ºC, with an additional shoulder at ~370ºC. The difference between these maxima and those recently reported by Frost and Ding (2003) may be due to the different

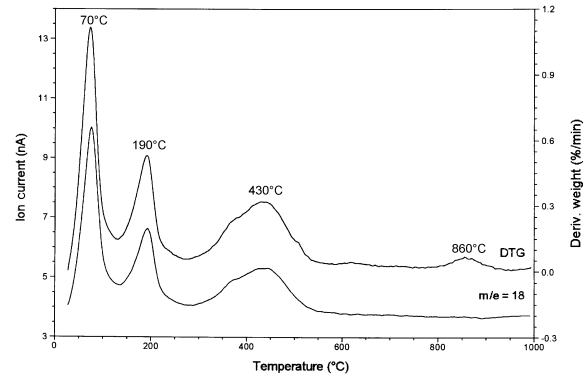

Figure 1. DTG and mass spectrometry of water (m/e = 18) of palygorskite heated from room temperature to 1000ºC in He with a ramp of 10ºC/min.

experimental conditions (rate of heating and nature and flow rate of the flowing gas). As a likely interpretation of the shoulder observed at 370ºC, the same authors have proposed that the completion of the dehydration at that temperature is accompanied by the folding of the tunnels. A partial dehydroxylation occurs at 430ºC and is completed at 860ºC (Frost and Ding, 2003). It has been proposed that the loss of the first structural water is accompanied by a partial collapse of the structure (Preisinger, 1963). This is apparent in Table 1: when the sample is heated at 300ºC for 20 h, the micropore area decreases from 93 m^2/g to 22 m^2/g, leaving unaffected the external surface area. Also shown in Table 1, the median pore diameter increases from 6.1 Å to 7.9 Å with the decrease of cumulative pore volume, because of the loss of the microporosity.

The nitrogen adsorption-desorption isotherm of PFl-1 is of type I at lower relative pressures, characteristic of microporous solids, and of type IV at higher relative pressures (Webb and Orr, 1997). This is in good agreement with previously reported measurements for palygorskite samples of other origins (Cases *et al*., 1991). A hysteresis is observed at higher relative pressures, indicative of the presence of interparticle mesopores. The BET surface area is 196 m^2/g, a value in good agreement with previously reported measurements for palygorskite samples of other origins (Barrer and Mackenzie, 1954: 195 m^2/g; Serna *et al*., 1977: 195 m^2/g; Gonzalez *et al*., 1989: 208 m^2/g; Suárez

Table 1. Textural analysis of palygorskite heated at various temperatures, and then degassed at room temperature.

Heating temperature	BET surface area (m^2/g)	T-plot			Horvath-Kawazoe	
		Micropore area (m^2/g)	External surface area (m^2/g)	Micropore volume (mm^3/g)	Cumulative pore volume (mm^3/g)	Median pore diameter (Å)
No heating	196	93	103	47	89	6.1
150ºC	206	93	113	46	93	6.2
200ºC	205	95	110	47	93	6.3
300ºC	130	22	108	10	55	7.9

https://doi.org/10.1346/CCMN.2004.0520509 Published online by Cambridge University Press

Barrios *et al*., 1995: 186 m^2/g). This measurement was confirmed by performing a congruent analysis using Ar as the adsorbed gas, yielding a BET surface measurement of 197±2 m^2/g. A t-plot analysis of the isotherm gives a micropore area of 93 m^2/g, a micropore volume of 47 mm^3/g (Table 1), and an external surface area of 103 m^2/g. Estimation of the micropore volume was enabled through desorption of the internal zeolitic water molecules during degassing.

Figure 2 shows the differential pore-volume plot of palygorskite (Horvath and Kawazoe, 1983), giving a median pore diameter of 6.1 Å (Table 1), with a sharp maximum at 4.9 Å**.** A median pore diameter of 6.3 Å is obtained for the sample heated up to 200ºC for 20 h, still keeping the microporosity of the original palygorskite sample. These values are in good agreement with the idealized crystallographic structure of palygorskite, and the dimension of its tunnels. Further heating at 300ºC produces a collapse of the structure as evidenced by the loss of microporosity, and a modification of the median pore diameter (7.9 Å) for the remaining micropores. As shown in Figure 2, the microporosity is almost completely lost for a palygorskite sample heated at 500ºC and then degassed at 200ºC.

^{29}Si NMR spectra of palygorskite

Figures 3a and 4a give the ^{29}Si MAS and CP/MAS NMR spectra of palygorskite, with two well-resolved resonances at −92.0 and −97.5 ppm. A significantly less intense resonance around −84.4 ppm is also observed. Barron and Frost (1985) reported the ^{29}Si MAS and CP/MAS NMR spectra of palygorskite, with two major resonances at −92 and −98 ppm, and a broad shoulder in the vicinity of −85 ppm. They assigned those resonances at −85, −92 and −98 ppm, respectively, to Q^2(Si-OH), to the center Si sites, and to the edge Si site. Different assignments of those resonances were reported later (Komarneni *et al*., 1986; d'Espinose de la Caillerie and Fripiat, 1994), under the assumption that for sepiolite and palygorskite, polarization transfer is possible only from the non-mobile protons of the structural water molecules and not from Mg-OH protons.

In a previous study (Weir *et al*., 2002), the ^{29}Si NMR signals of sepiolite were assigned with the aid of two-dimensional ^{29}Si COSY and ^{1}H-^{29}Si heteronuclear correlation (HETCOR) NMR pulse sequences. It was shown that the Mg-OH protons are principally responsible for the polarization transfer to ^{29}Si, and conse-

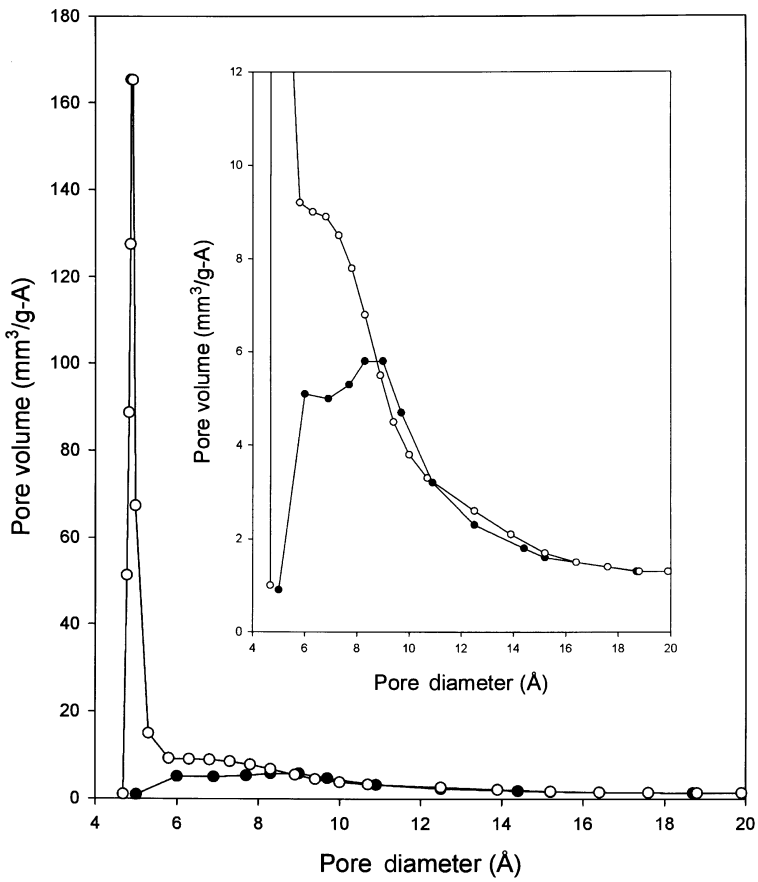

Figure 2. Horvath-Kawazoe differential pore-volume plot of palygorskite degassed at room temperature (open circles) and of palygorskite heated at 500ºC then degassed at 200ºC (filled circles).

https://doi.org/10.1346/CCMN.2004.0520509 Published online by Cambridge University Press

quently for the increase of intensity observed for the ^{29}Si NMR signals of the Si atoms close to the Mg-OH unit.

Due to the existence of relatively large amounts of Fe, the ^{1}H NMR spectrum of the palygorskite sample is composed of a series of very broad and strongly overlapping peaks (see Figure 5a). It is thus not possible to apply 2D techniques for an unambiguous assignment of the two palygorskite ^{29}Si NMR peaks. Moreover, the ^{29}Si NMR signals of palygorskite are much weaker than those of sepiolite.

A comparison of the ^{29}Si MAS and CP/MAS NMR spectra shown in Figures 3 and 4, repectively, permits us to assign the resonance at −92.0 ppm to the center Si nuclei, which are located very close to the Mg-OH groups and are expected to cross-polarize efficiently with the hydroxyl protons. The resonance at −97.5 ppm can be assigned to the edge Si nuclei, situated further away from the Mg-OH groups.

By analogy with sepiolite (Weir *et al*., 2002), the signal at −84.4 ppm can be assigned to the Q^2(SiOH) Si site. The ^{29}Si MAS NMR spectrum of palygorskite given in Figure 3a is quantitative, and the integral ratio is ~1:7:6 for the resonances at −84.4, −92.0 and −97.5 ppm, respectively. The sum of the integrals of the resonances at −84.4 and at −97.5 ppm is equal to the integral for the resonance at −92.0 ppm. Since the edge Si is replaced by Q^2(SiOH) at the borders of external surfaces, the sum of the integrals of the edge and of the Q^2 resonances should be equal to the integrals for the center signals. This is an additional argument to assign the resonances at −92.0, and −97.5 ppm to the center and edge silicon nuclei, respectively. The experimental quantitative ratio of Q^2 over Q^3 is 1:13, in excellent agreement with the morphology model of palygorskite proposed by Serna and VanScoyoc (1979), giving an idealized ratio of 1:14. This result also indicates that ~8% of the silicon nuclei in palygorskite exist as SiOH groups.

^{29}Si NMR spectra of partially dehydrated palygorskite

The ^{29}Si MAS and CP/MAS NMR spectra of palygorskite previously heated in air at 150 and 300ºC are presented in Figures 3(b,c) and 4(b,c), respectively. The ^{29}Si NMR spectra are sensitive to the changes in the palygorskite structure occurring when zeolitic water molecules are removed from the tunnels. After heating at 150ºC for 20 h, the two main resonances shift to −93.1, and −96.9 ppm, respectively. As mentioned above, only the mobile zeolitic water molecules are removed after heating at 150ºC for 20 h, while the Mg-OH groups and the coordinated water molecules remain in the structure. After heating at 300ºC for 20 h, the resonances overlap,

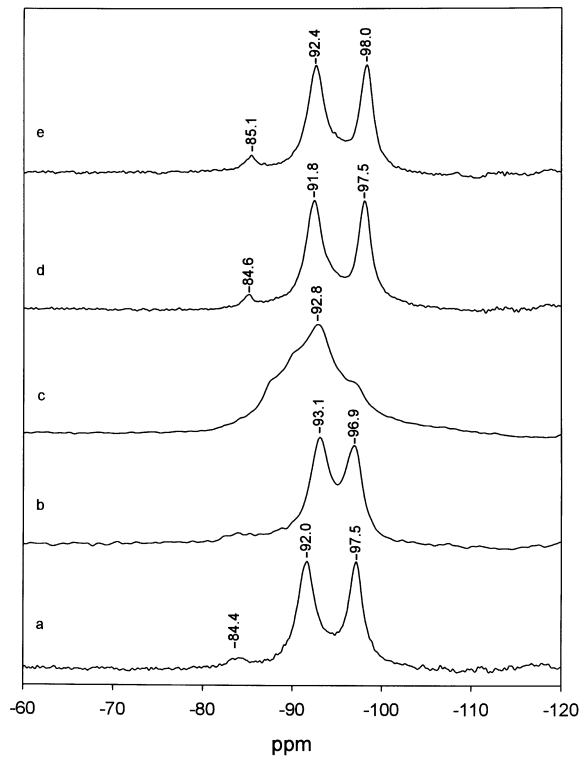

Figure 3. ^{29}Si MAS NMR spectra of samples: (a) palygorskite; (b) palygorskite heated at 150ºC for 20 h; (c) palygorskite heated at 300ºC for 20 h; (d) palygorskite heated at 150ºC for 20 h then exposed to D_2O; (e) palygorskite heated at 300ºC for 20 h then exposed to D_2O.

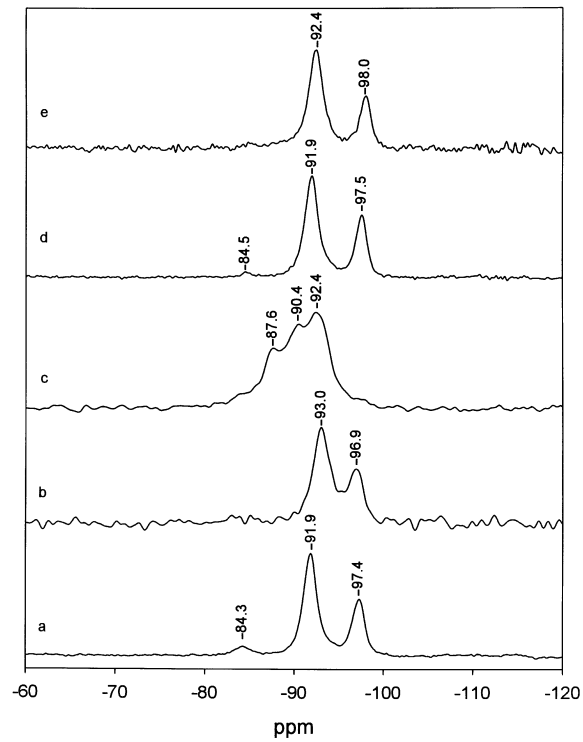

Figure 4. ^{29}Si CP/MAS NMR spectra of samples: (a) palygorskite; (b) palygorskite heated at 150ºC for 20 h; (c) palygorskite heated at 300ºC for 20 h; (d) palygorskite heated at 150ºC for 20 h then exposed to D_2O; (e) palygorskite heated at 300ºC for 20 h then exposed to D_2O.

https://doi.org/10.1346/CCMN.2004.0520509 Published online by Cambridge University Press

giving several broad signals, with a peak maximum around −92.8 ppm. This results from the partial removal of structural water molecules from the coordination shell of the edge cations and the folding of the palygorskite structure, with a loss of symmetry causing unresolved multiplicity of the Si sites.

Rehydration of palygorskite previously heated to 150ºC and 300ºC

As discussed above, after heating at 150ºC for 20 h, the zeolitic water molecules are selectively removed, the microporosity is maintained, the tunnels remain accessible, and the presence of the structural water molecules coordinated to terminal Mg(II) prevents folding of the structure. Heating at 300ºC for 20 h produces a folding of the structure due to the partial removal of the structural water molecules. The microporosity of the material is then largely lost.

The ^{29}Si MAS and CP/MAS-NMR spectra of a partially dehydrated palygorskite sample subsequently exposed to D_2O vapor are shown in Figures 3(d,e) and 4(d,e). They are almost identical to the spectra of the original clay mineral, indicating that exposure to D_2O vapor restores the original structure when palygorskite was previously heated at 150 or 300ºC. This implies that the D_2O molecules have filled the microporous tunnels and reversed the structural changes that were caused by partial dehydration. Heating to 150ºC for 20 h results in a partially dehydrated clay mineral in which the microporous tunnels are accessible to D_2O. In the case of heating to 300ºC for 20 h, despite the observed folding of palygorskite and the concurrent loss of microporosity, D_2O molecules can access the interior of the structure, restoring the nanotunnel structure, in a perfectly reversible manner. This reversibility was not observed when palygorskite was heated at 400ºC for 20 h, a temperature at which the second structural water is also removed and some partial dehydroxylation can occur. At this temperature, the folding appears to be irreversible.

The relative intensities of the two peaks in the CP/MAS spectrum are identical to those of the original sample. This shows that, upon rehydration with D_2O, the D atoms are scrambled across the various proton sites, zeolitic water, coordinated water and hydroxyls, in a statistical manner. As a result, the distribution of ^{1}H in the structure is identical for the original and for the D_2O-exchanged samples, resulting in equivalent relative cross-polarization effects on the two sites. This H-D exchange was also shown by IR spectroscopy (Serna *et al*., 1977).

Figure 5 gives the corresponding ^{1}H NMR spectra. While the spectrum is characterized by very broad lines in the original palygorskite sample, the removal of the zeolitic water molecules results in a much better-resolved spectrum. Two signals are apparent, with an intense set of spinning side bands. This spectrum is similar to that reported for sepiolite (Weir *et al*., 2002). The resonance at lower frequency produces only a few spinning side bands, and can be attributed to Mg-OH groups, while the resonance at higher frequency can be attributed to structural water. The spectra are similar when the palygorskite sample is heated at 150ºC and at 300ºC. Upon exposure to D_2O, a strong signal with no spinning side bands develops. It can be attributed to the mobile, zeolitic water. Upon rehydration with D_2O, protons and deuterons undergo statistical exchange among the various proton sites, resulting in a large proton signal for the zeolitic water. The peak of the hydroxyl groups can be observed as a shoulder at lower frequency. The dilution of the ^{1}H nuclei in the D_2O-exchanged palygorskite results in a spectrum (Figure 5f) better resolved than the spectrum of the original palygorskite sample (Figure 5a) due to significantly reduced dipolar interactions between protons which can be more easily averaged by magic angle spinning.

This study confirms that the dehydration of palygorskite is fully reversible when it is heated at temperatures up to 300ºC, even if, at that temperature, ~50% of the structural water molecules have been removed, causing a folded structure with an associated loss in microporosity. ^{29}Si solid-state NMR proves to be a very sensitive probe of the structural changes of

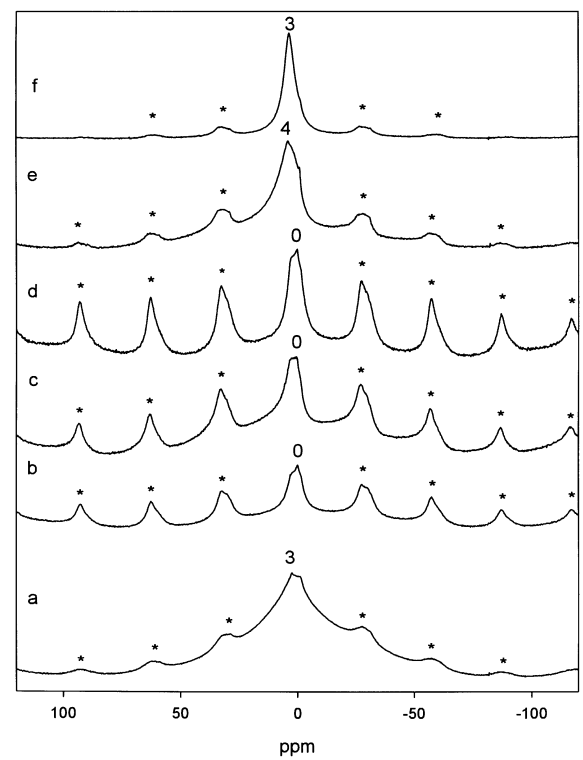

Figure 5. ^{1}H MAS NMR spectra of samples: (a) palygorskite; (b) palygorskite heated at 100ºC for 20 h; (c) palygorskite heated at 150ºC for 20 h; (d) palygorskite heated at 300ºC for 20 h; (e) sample d exposed to D_2O for one week; (f) sample d exposed to D_2O for 3 months. * denotes spinning side bands.

https://doi.org/10.1346/CCMN.2004.0520509 Published online by Cambridge University Press

palygorskite and sepiolite, and is particularly responsive to the filling of the tunnels by water molecules as shown in this work, or by organic molecules as shown previously in the cases of acetone (Weir *et al*., 2000) and pyridine (Kuang *et al*., 2003).

CONCLUSIONS

The TGA-MS clearly shows four major weight-loss events of PFl-1 at maxima of 70ºC, 190ºC, 430ºC and 860ºC, attributed to the release of zeolitic water, the release of the first structural water, the release of the second structural water, and the dehydroxylation of the Mg-OH groups, respectively. The nitrogen adsorption-desorption isotherm of PFl-1 is of type I at lower relative pressures, characteristic of microporous solids. The BET surface area is 196 m^2/g, with a micropore area of 93 m^2/g, a micropore volume of 47 mm^3/g, and an external surface area of 103 m^2/g. The differential pore-volume plot of palygorskite, reveals a median pore diameter of 6.1 Å, with a sharp maximum at 4.9 Å. By analogy with sepiolite, a comparison of the ^{29}Si MAS and CP/MAS NMR spectra indicates the assignment of the resonance at −92.0, −97.5 and −84.4 ppm to the center Si nuclei, to the edge Si nuclei, and to the Q^2(SiOH) Si site, respectively. Approximately 8% of the Si nuclei in PFl-1 exist as SiOH groups. The ^{29}Si and ^1H NMR spectra indicate that exposure to D_2O or water vapor at room temperature restores the original structure when palygorskite was previously heated at 150ºC or 300ºC. The D_2O molecules can access the interior of the structure, restoring the nanotunnel structure. Upon rehydration with D_2O, the D atoms are scrambled across the various proton sites, zeolitic water, coordinated water and hydroxyls, in a statistical manner.

ACKNOWLEDGMENTS

The Natural Sciences and Engineering Research Council of Canada (NSERC, discovery grant program) is thanked for financial support.

REFERENCES

Artioli, G. and Galli, E. (1994) The crystal structures of orthorhombic and monoclinic palygorskite. *Materials Science Forum*, **166–169**, 647–652.

Artioli, G., Galli, E., Burattini, E., Cappuccio, G. and Simeoni, S. (1994) Palygorskite from Bolca, Italy: a characterization by high-resolution synchrotron radiation powder diffraction and computer modeling. *Neues Jahrbuch für Mineralogie, Monatshefte*, 217–229.

Augsburger, M.S., Strasser, E., Perino, E., Mercader, R.C. and Pedregosa, J.C. (1998) FTIR and Mössbauer investigation of a substituted palygorskite: silicate with a channel structure. *Journal of Physics and Chemistry of Solids*, **59**, 175–180.

Barrer, R.M. and Mackenzie, N. (1954) Sorption by attapulgite. I. Availability of intracrystalline channels. *Journal of Physical Chemistry*, **58**, 560–568.

Barron, P.F. and Frost, R.L. (1985) Solid-state ^{29}Si NMR examination of the 2:1 ribbon maganesium silicates, sepiolite and palygorskite. *American Mineralogist*, **70**, 758–766.

Birsoy, R. (2002) Formation of sepiolite-palygorskite and related minerals from solution. *Clays and Clay Minerals*, **50**, 736–745.

Borden, D. and Giese, R.F. (2001) Baseline studies of the Clay Minerals Society source clays: cation exchange capacity measurements by the ammonia-electrode method. *Clays and Clay Minerals*, **49**, 444–445.

Bradley, W.F. (1940) The structural scheme of attapulgite. *American Mineralogist*, **25**, 405–410.

Cases, J.M., Grillet, Y., Francois, M., Michot, L., Villieras, F. and Yvon, J. (1991) Evolution of the porous structure and surface area of palygorskite under vacuum thermal treatment. *Clays and Clay Minerals*, **39**, 191–201.

Chahi, A., Petit, S. and Decarreau, A. (2002) Infrared evidence of dioctahedral-trioctahedral site occupancy in palygorskite. *Clays and Clay Minerals*, **50**, 306–313.

Chiari, G., Giustetto, R. and Ricchiardi, G. (2003) Crystal structure refinements of palygorskite and Maya Blue from molecular modelling and powder synchrotron diffraction. *European Journal of Mineralogy*, **15**, 21–33.

Chipera, S.J. and Bish, D.L. (2001) Baseline studies of the Clay Minerals Society source clays: powder X-ray diffraction analyses. *Clays and Clay Minerals*, **49**, 398–409.

Chisholm, J.E. (1990) An X-ray powder-diffraction study of palygorskite. *The Canadian Mineralogist*, **28**, 329–339.

Chisholm, J.E. (1992) Powder-diffraction patterns and structural models for palygorskite. *The Canadian Mineralogist*, **30**, 61–73.

Costanzo, P.M. and Guggenheim, S., editors (2001) Baseline studies of the Clay Minerals Society source clays. *Clays and Clay Minerals*, **49**, 371–452.

d'Espinose de la Caillerie, J.-B. and Fripiat, J.J. (1994) A reassessment of the ^{29}Si MAS-NMR spectra of sepiolite and aluminated sepiolite. *Clay Minerals*, **29**, 313–318.

Fernandez, M.E., Ascencio, J.A., Mendoza-Anaya, D., Rodriguez Lugo, V. and Jose-Yacaman, M. (1999) Experimental and theoretical studies of palygorskite clays. *Journal of Materials Science*, **34**, 5243–5255.

Fois, E., Gamba, A. and Tilocca, A. (2003) On the unusual stability of Maya blue paint: molecular dynamics simulations. *Microporous and Mesoporous Materials*, **57**, 263–272.

Frost, R.L. and Ding, Z. (2003) Controlled rate thermal analysis and differential scanning calorimetry of sepiolites and palygorskites. *Thermochimica Acta*, **397,** 119–128.

Frost, R.L., Cash, G.A. and Kloprogge, J.T. (1998) 'Rocky Mountain leather', sepiolite and attapulgite – an infrared emission spectroscopic study. *Vibrational Spectroscopy*, **16**, 173–184.

Frost, R.L., Locos, O.B., Ruan, H. and Kloprogge, J.T. (2001) Near-infrared and mid-infrared spectroscopic study of sepiolites and palygorskites. *Vibrational Spectroscopy*, **27**, 1–13.

Galán, E. (1996) Properties and applications of palygorskite-sepiolite clays. *Clay Minerals*, **31**, 443–453.

Galán, E. and Carretero M.I. (1999) A new approach to compositional limits for sepiolite and palygorskite. *Clays and Clay Minerals*, **47**, 399–409.

Gonzalez, F., Pesquera, C., Blanco, C., Benito, I., Mendioroz, S. and Pajares, J.A. (1989) Structural and textural evolution of Al- and Mg-rich palygorskites, I. Under acid treatment. *Applied Clay Science*, **4**, 373–388.

Guggenheim, S. and Koster van Groos, A.F. (2001) Baseline studies of the Clay Minerals Society source clays: thermal analysis. *Clays and Clay Minerals*, **49**, 433–443.

Güven, N., d'Espinose de la Caillerie, J.-B. and Fripiat, J.J. (1992) The coordination of aluminum ions in the palygorskite structure. *Clays and Clay Minerals*, **40**, 457–461.

Horvath, G. and Kawazoe, K. (1983) Method for the calculation of effective pore size distribution in molecular sieve carbon. *Journal of Chemical Engineering of Japan,* **16**, 470–475.

Hubbard, B., Kuang, W., Moser, A., Facey, G.A. and Detellier, C. (2003) Structural study of Maya blue: textural, thermal and solid state multinuclear magnetic resonance characterization of the palygorskite-indigo and sepiolite-indigo adducts. *Clays and Clay Minerals*, **51**, 318–326.

Jones, B.F. and Galán, E. (1988) Sepiolite and palygorskite. Pp. 631–674 in: *Hydrous Phyllosilicates* (S.W. Bailey, editor). Reviews in Mineralogy, **19**, Mineralogical Society of America, Washington, D.C.

Kleber, R., Masschelein-Kleiner, L. and Thissen, J. (1967) Study and identification of Maya blue. *Studies in Conservation*, **12**, 41–56.

Komarneni, S., Fyfe, C.A. and Kennedy, G.J. (1986) Detection of nonequivalent Si sites in sepiolite and palygorskite by solid-state ^{29}Si Magic Angle Spinning-Nuclear Magnetic Resonance. *Clays and Clay Minerals*, **34**, 99–102.

Kuang, W., Facey, G.A., Detellier, C., Casal, B., Serratosa, J.M. and Ruiz-Hitzky, E. (2003) Nanostructured hybrid materials formed by sequestration of pyridine molecules in the tunnels of sepiolite. *Chemistry of Materials*, **15**, 4956–4967.

Madejová, J. and Komadel, P. (2001) Baseline studies of the Clay Minerals Society source clays: infrared methods. *Clays and Clay Minerals*, **49**, 410–432.

McKeown, D.A., Post, J.E. and Etz, E.S. (2002) Vibrational analysis of palygorskite and sepiolite. *Clays and Clay Minerals*, **50**, 667–680.

Mermut, A.R. and Cano, A.F. (2001) Baseline studies of the Clay Minerals Society source clays: chemical analysis of major elements, *Clays and Clay Minerals*, **49**, 381–386.

Murray, H.H. (1991) Overview – clay mineral applications. *Applied Clay Science*, **5**, 379–395.

Murray, H.H. (1999) Applied clay mineralogy today and tomorrow. *Clay Minerals*, **34**, 39–49.

Murray, H.H. (2000) Traditional and new applications for kaolin, smectite, and palygorskite: a general overview. *Applied Clay Science*, **17**, 207–221.

Polette, L.A., Meitzner, G., Yacamán, M.J. and Chianelli, R.R. (2002) Maya blue: application of XAS and HRTEM to materials science in art and archaeology. *Microchemical Journal*, **71**, 167–174.

Preisinger, A. (1963) Sepiolite and related compounds: its stability and application. *Clays and Clay Minerals*, **10**, 365–371.

Sanz, J. (1990) Distribution of ions in phyllosilicates by NMR spectroscopy. Pp 103–144 in: *Absorption Spectroscopy in Mineralogy* (A. Moltana and F. Burragato, editors). Elsevier, Amsterdam.

Serna, C.J. and VanScoyoc, G.E. (1979) Infrared study of sepiolite and palygorskite surfaces. Pp 197–206 in: *Proceedings of the International Clay Conference*, *Oxford*, 1978. Elsevier, Amsterdam.

Serna, C., VanScoyoc, G.E. and Ahlrichs J.L. (1977) Hydroxyl groups and water in palygorskite. *American Mineralogist*, **62**, 784–792.

Serratosa, J.M. (1979) Surface properties of fibrous clay minerals (palygorskite and sepiolite). Pp. 99–109 in: *Proceedings of the International Clay Conference*, *Oxford, 1978*. Elsevier, Amsterdam.

Shariatmadari, H., Mermut, A.R. and Benke, M.B. (1999) Sorption of selected cationic and neutral organic molecules on palygorskite and sepiolite. *Clays and Clay Minerals*, **47**, 44–53.

Shore, J.S., DePaul, S., Ernst, M. and Phillips, B.L. (1998) Double-resonance and two-dimensional Silicon-29 NMR spectroscopy of minerals. Pp. 305–325 in: *Solid-State Nuclear Magnetic Resonance of Inorganic Materials* (J.J. Fitzgerald, editor). ACS Symposium Series, **717**, American Chemical Society.

Shuali, U., Yariv, S., Steinberg, M., Muller-Vonmoos, M., Kahr, G. and Rub, A. (1988) Thermal analysis study of the adsorption of heavy water by sepiolite and palygorskite. *Thermochimica Acta*, **135**, 291–297.

Shuali, U., Steinberg, M., Yariv, S., Muller-Vonmoos, M., Kahr, G. and Rub, A. (1990) Thermal analysis of sepiolite and palygorskite treated with butylamine. *Clay Minerals*, **25**, 107–119.

Sidheswaran, P. (2002) Heat-induced structural modifications in palygorskite. *Clay Research*, **21**, 27–39.

Suárez Barrios, M., Flores González, L.V., Vicente Rodríguez, M.A. and Martín Pozas, J.M. (1995) Acid activition of a palygorskite with HCl: development of physico-chemical, textural and surface properties. *Applied Clay Science*, **10**, 247–258.

van Olphen, H. (1966) Maya Blue: a clay mineral-organic pigment? *Science*, **154**, 645–646.

van Olphen, H. and Fripiat, J.J. (1979) *Data Handbook for Clay Materials and Other Non-Metallic Minerals*. Pergamon Press, Oxford, England, 346 pp.

VanScoyoc, G.E., Serna, C.J. and Ahlrichs J.L. (1979) Structural changes in palygorskite during dehydration and dehydroxylation. *American Mineralogist*, **64**, 215–223.

Webb, P.A. and Orr, C. (1997) *Analytical Methods in Fine Particle Technology*. Micromeritics Instrument Corporation, Norcross, Georgia, 301 pp.

Weir, M.R., Facey, G.A. and Detellier, C. (2000) ^{1}H, ^{2}H, and ^{29}Si solid state NMR study of guest acetone molecules occupying the zeolitic channels of partially dehydrated sepiolite clay. *Studies in Surface Science and Catalysis*, **129**, 551–558.

Weir, M.R., Kuang, W., Facey, G.A. and Detellier, C. (2002) Solid state nuclear magnetic resonance study of sepiolite and partially dehydrated sepiolite. *Clays and Clay Minerals*, **50**, 240–247.

Wu, W. (2001) Baseline studies of the Clay Minerals Society source clays: Colloid and surface phenomena. *Clays and Clay Minerals*, **49**, 446–452.

Yacamán, M.J., Rendon, L., Arenas, J. and Puche, M.C.S. (1996) Maya blue paint: an ancient nanostructured material. *Science*, **273**, 223–225.

(*Received 1 December 2003; revised 21 April 2004; Ms. 861; A.E. Randall T. Cygan*)